

STRUCTURAL DAMAGE DETECTION THROUGH CROSS CORRELATION ANALYSIS OF MOBILE SENSING DATA

Dapeng Zhu, Xiaohua Yi, Yang Wang¹

School of Civil and Environmental Engineering, Georgia Institute of Technology, Atlanta, GA 30332, USA

¹yang.wang@ce.gatech.edu

Karim Sabra

School of Mechanical Engineering, Georgia Institute of Technology, Atlanta, GA 30332, USA

karim.sabra@me.gatech.edu

Abstract

This paper describes the application of cross-correlation function for structural damage detection, using vibration data collected by a previously developed mobile sensor prototype. A damage indicator is defined by comparing the peak amplitude of the cross correlation function of the damaged structure versus the undamaged structure. Laboratory experiments are conducted to validate the damage detection approach. Mobile sensing nodes navigating on a steel portal frame are used to collect the vibration data with high spatial resolution. Various damage scenarios have been investigated, including extra mass, loosened bolts, and loss of section area. It is shown the cross correlation analysis using mobile sensing data can both identify and locate damage in a portal frame structure.

Introduction

Due to various adverse operational and environmental conditions, civil structures may deteriorate rapidly during its life span. For example, more than a quarter of the bridges in United States were categorized as structurally deficient or functionally obsolete. It was estimated that a \$17 billion annual investment is need to substantially improve current conditions; however, only \$10.5 billion is available annually on the construction and maintenance of bridges (ASCE 2009). To efficiently utilize limited resources, it is essential to make accurate evaluation of civil structures' safety conditions. Significant research efforts have been devoted to structural health monitoring (SHM) systems that are promising in closely monitoring structural conditions. For example, various academic and industrial wireless sensing prototypes have been developed and validated in order to reduce the high cost of traditional cable-based structural monitoring systems (Lynch and Loh 2006).

As a transformative change to wireless sensing, mobile sensing systems containing mobile sensing nodes offer flexible system architectures and adaptive spatial resolutions (Akyildiz *et al.* 2002). In robotics field, many efforts have been made in incorporating mobility into traditional sensors. For example, based upon magnetic on-off robotic attachment devices, a magnetic walker has been developed for maneuvering on a 2D surface (Brian *et al.* 2004). In order to inspect the inner casing of ferromagnetic pipes, a compact robot with two magnetic wheels in a motorbike arrangement has been developed; the robot can slightly lift off the wheel in order to negotiate concave edges (Tache *et al.* 2009). In the SHM field, most recently, Lee *et al.* (2009) and Zhu *et al.* (2010) presented a flexure-based mechatronic (flexonic) mobile sensing node, which is capable of attaching/detaching an accelerometer onto/from the structural surface. Meanwhile, this flexonic mobile sensing node has the potential to fulfill functions of negotiating in complex steel structures with narrow sections and high abrupt angle changes. The flexonic mobile sensing nodes are used in this work for collecting vibration data from a laboratory structure.

In recent years, a myriad of vibration-based damage detection methods have been developed. The methods can be categorized into two groups: model-based approaches and non-model-based approaches (Doebbling *et al.* 1998). Model-based approaches aim to update corresponding finite element models based on the differences between the measurement and the prediction by the finite element models. If the measurement resolutions are relative low or the initial finite element models are not accurate enough, model-based approaches might encounter convergence problems. As a complement to the model-based

approaches, non-model approaches may avoid such convergence difficulties. Among various non-model approaches, this work investigates the cross-correlation analysis for detecting structural damage.

Cross correlation analyses have been recently explored for structural health monitoring and damage detection. Farrar and James (1997) proved that the cross-correlation functions of the responses excited by ambient noise have similar characteristics as the structural impulse response functions, and can be adopted for identifying structural dynamic properties. Lin *et al.* (2005) studied the Hilbert–Huang transform of the cross correlation functions to identify the damage on a benchmark building. Sabra *et al.* (2007) investigated cross correlation analysis using random vibration data recorded in the test section of a large cavitation channel; deterministic time signatures are extracted from the noise cross-correlation function. Yang *et al.* (2007) validated the cross correlation function analysis for damage detection of a laboratory composite beam under random excitation. This paper investigates deterministic cross correlation analysis of vibration data collected by mobile sensors from a structure under hammer excitation.

In our previous research, transmissibility analysis using mobile sensing data has been illustrated to successfully detect structural damages in laboratory experiments (Zhu *et al.* 2010). As a continuing effort, cross correlation function analyses using mobile sensing data is studied in this paper. The paper begins with the formulation of cross correlation analysis. Laboratory validation experiments with three damage scenarios are then presented, and followed by the damage detection results using the data collected by the mobile sensors.

Damage Indicator Based upon Cross Correlation Function

Consider a structure under single-point hammer impact excitation, the deterministic cross correlation function between the response at the i -th and j -th DOFs (degrees of freedom) is given by

$$R_{ij}(\tau) = \lim_{T \rightarrow \infty} \frac{1}{T} \int_0^T a_i(t + \tau) a_j(t) dt \quad (1)$$

where $a_i(t)$ represents the acceleration measurement at DOF i . The time-discretized version of the cross-correlation function is defined as

$$R_{ij}(k) = \begin{cases} \frac{1}{N_0 - k} \sum_{n=0}^{N_0-k-1} a_i(n+k) a_j(n) & k \geq 0 \\ R_{ji}(-k) & k < 0 \end{cases} \quad (2)$$

where $\tau = k\Delta$, and Δ is the sampling period. N_0 denotes the length of the measurement data.

The deterministic correlation function can be normalized by

$$\tilde{R}_{ij}(k) = \frac{R_{ij}(k)}{\sqrt{R_{ii}(0)} \sqrt{R_{jj}(0)}} \quad (3)$$

Under hammer impact excitation, the cross-correlation functions are determined by the impulse responses that correspond to inherent dynamics properties of the structure. After damage occurs, the impulse response functions change. Therefore, by comparing the cross-correlation functions of the undamaged structure and damaged structure, damage can be identified. In this work, the maximum absolute values of the normalized deterministic cross-correlation functions are used for comparison, which is denoted as r_{ij} :

$$r_{ij} = \max_k (|\tilde{R}_{ij}(k)|) \quad (4)$$

It is known that r_{ij} has a value between 0 and 1, and measures the similarity between the two acceleration records, $a_i(t)$ and $a_j(t)$. When the two acceleration records are more similar to each other, r_{ij} is closer to 1. If damage occurs near two DOFs i and j , it is likely that r_{ij} of the damaged structure is different from the r_{ij} of the undamaged structure. The damage indicator (DI) between DOF i and DOF j is defined as

$$DI_{ij} = \frac{|r_{ij}^D - r_{ij}^U|}{r_{ij}^U} \quad (5)$$

where superscript U and D represent the undamaged structure and the damaged structure, respectively. r_{ij}^U represent the maximum absolute values of the normalized deterministic cross correlation functions for the undamaged structure, and r_{ij}^D represents this for the damaged structure.

In order to reduce the effect of experimental uncertainties, the measurement at each configuration is repeated for N times for both the undamaged and damaged structures. Damage indicator is then calculated as following, using the averaged maximum absolute values of the normalized deterministic cross correlation functions:

$$r_{ij}^U = \frac{1}{N} \sum_{k=1}^N (r_{ij}^U)_k \quad (6a)$$

$$r_{ij}^D = \frac{1}{N} \sum_{k=1}^N (r_{ij}^D)_k \quad (6b)$$

where subscript k represents the k -th repeating test.

Furthermore, repeatability check can be performed to ensure that experimental uncertainties, including sensor noise and the application of external input, have negligible influence to the damage detection results. For either an undamaged or a damaged structure, the N data sets are separated into two groups of $N/2$ data sets. One group may consist of data with odd sequence numbers, and the other one consists of data with even sequence numbers. Taking the undamaged structure as an example, the averaged maximum absolute values of the normalized deterministic cross correlation functions for each data group is calculated by:

$$r_{ij}^{U_odd} = \frac{2}{N} \sum_{k=1}^{N/2} (r_{ij}^U)_{2k-1} \quad (7a)$$

$$r_{ij}^{U_even} = \frac{2}{N} \sum_{k=1}^{N/2} (r_{ij}^U)_{2k} \quad (7b)$$

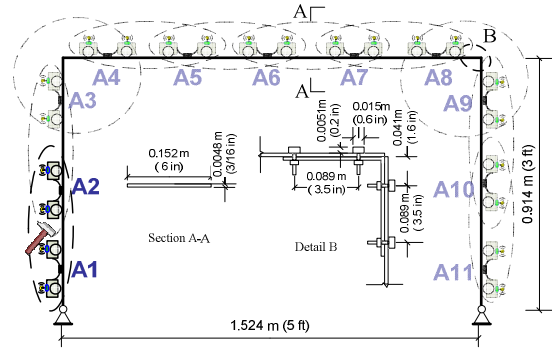
The repeatability indicator (RI) is then defined in a similar form to the damage indicator. For the experiments with undamaged structure, the repeatability indicator for DOF pair i and j is defined as:

$$RI_{ij}^U = \frac{|r_{ij}^{U_odd} - r_{ij}^{U_even}|}{r_{ij}^{U_odd}} \quad (8)$$

Note that a smaller repeatability indicator RI represents a higher level of repeatability. Similarly, the repeatability indicator for experiments with the damaged structure, RI_{ij}^D , can be calculated.



(a)



(b)

Figure 1. Laboratory steel portal frame for damage detection using mobile sensors: (a) picture of the portal frame with mobile sensors at A1 and A2; (b) schematic of experimental setup.

It should also be noted that this damage detection method is not constrained to hammer excitation. When the structure is excited by white noise input, probabilistic cross correlation analysis for damage detection can be conducted in a similar fashion.

Laboratory Experiments

This section first introduces the laboratory structure and data collection for damage detection experiments. Three damage scenarios and corresponding damage detection results are then presented: the first scenario simulated with an extra mass block, the second scenario simulated with loosened bolts, and the third scenario simulated with loss of section area in one column.

Laboratory Setup and Data Collection

A laboratory steel portal frame is constructed for investigating cross correlation analysis using the mobile sensors (Figure 1(a)). The span of the portal frame is 1.524m (5 ft), and the height is 0.914m (3 ft). The beam and two columns have the same rectangular section area of 0.152m (6 in) \times 0.005m (3/16 in). Hinge connections are adopted at the bases of the two columns. Each column is connected with the beam through an angle plate, with 4 bolts on the beam and 4 bolts on the column. The torque of each bolt is initially set at 13.56Nm (120 lbs-in) for the undamaged structure.

Mobile sensors, which are capable of moving on the steel structure as well as attaching/detaching an accelerometer (Silicon Designs 2260-010) onto/from structural surface, are used in the experiments. The design and implementation of the mobile sensor can be found in Zhu *et al.* (2010). As shown in Figure 1 (b), two mobile sensors are adopted to take measurement at every pair of locations (A1-A2, A2-A3, ..., A10-A11), sequentially. In the experiments, when the two mobile sensors arrive at one pair of measurement locations, the accelerometer is attached onto the structural surface; then a hammer impact is applied at the middle of these two adjacent measurement locations. After the measurement, these two mobile sensors detach accelerometers from structural surface, and move to next pair of measurement locations. In order to reduce the effect of experimental uncertainties, measurement at each location pairs is repeatedly taken for 20 times, i.e. $N = 20$ in Eq. (6). The sampling rate for the acceleration measurement is set to 2500 Hz.

Figure 2(a) plots the acceleration data at location A1 and Figure 2(b) plots the acceleration data at location A2. Both data sets are simultaneously collected when an impact hammer hits between A1 and A2. Figure 3 shows the normalized deterministic cross correlation function calculated from the

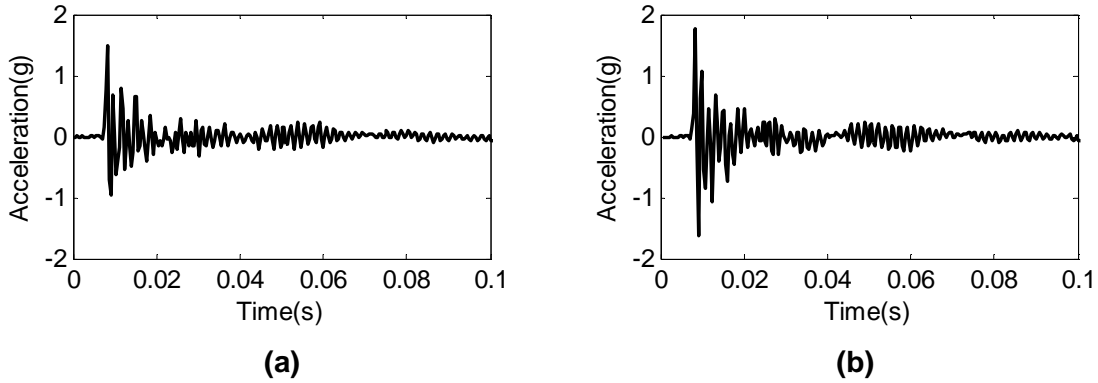


Figure 2. Acceleration data recorded by mobile sensors: (a) location A1; (b) location A2. Hammer impact is applied between A1 and A2 (as shown in Figure 1).

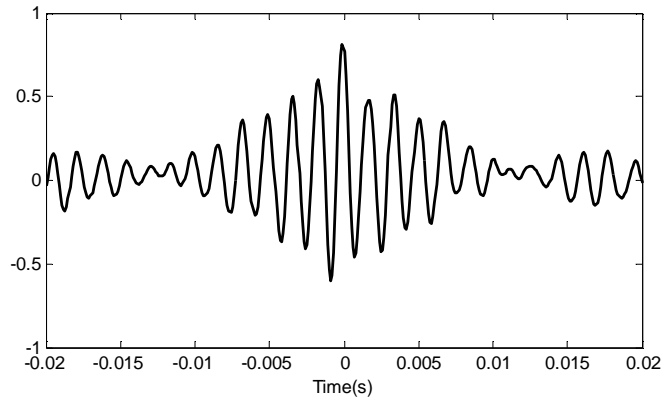


Figure 3. The normalized deterministic cross correlation function calculated from the acceleration data at location A1 and A2.

acceleration data of locations A1 and A2, following Eq. (2). As expected, the peak absolute value, r_{12} , is between 0 and 1.

Damage Scenario I – Extra Mass Block

In Damage Scenario I, a steel mass block of 0.575 kg (1.27 lbs) is bonded to the left column for simulating a reversible damage (Figure 4). In contrast, the mass of the left column is 4.985 kg (10.99 lbs). The bonding location is at 0.229 m (9 in) above the column base, which is between locations A1 and A2. Same as the measurement scheme for the undamaged structure, the two mobile sensors take measurement at location pairs A1-A2, A2-A3, ..., and A10-A11, sequentially. At each location pair, measurement is repeated for 20 times. Using all the experimental data sets for both the undamaged and damaged structures, the averaged maximum absolute values of the normalized deterministic cross correlation functions of each location pair, r_{ij}^U and r_{ij}^D , are computed according to Eq. (6). Then damage indicators are calculated following Eq. (5). As presented in Figure 5, the largest damage indicator is $DI_{1-2} = 0.12$, which agrees with the correct damage location, i.e. between locations A1 and A2 (Figure 1). For each location pair in Figure 5, a positive (+) or a negative (-) sign is placed on top of the bar corresponding to the damage indicator. The sign demonstrates the change in the maximum absolute value of the cross correlation function from the undamaged to the damaged case, i.e. same as the sign of $r_{ij}^D - r_{ij}^U$. At the



Figure 4. Damage Scenario I - an extra mass block mounted between locations A1 and A2.

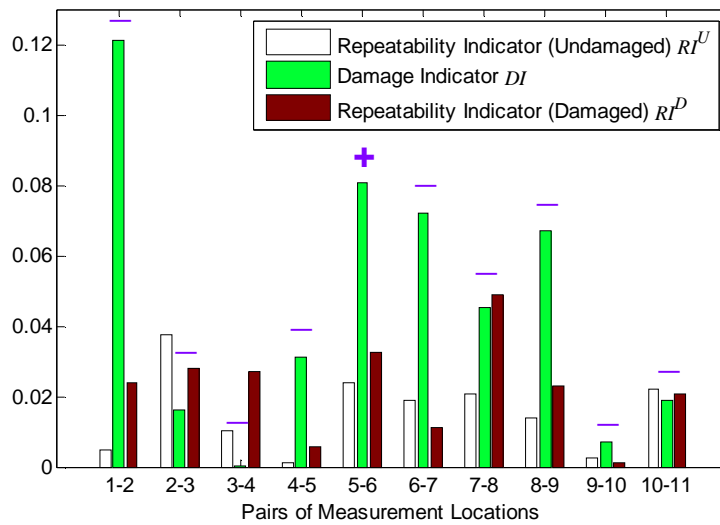


Figure 5. Damage Scenario I - the damage indicators and repeatability indicators for ten pairs of measurement locations. The sign of $r_{ij}^D - r_{ij}^U$ for each location pair is shown above the bar corresponding to the Damage Indicator DI .

damage location, the negative sign shows that after damage occurs, less similarity exists between the hammer impact responses at location A1 and location A2.

In order to verify the experimental repeatability, for the undamaged structure, the 20 data sets at each location pair are separated into an odd-sequence group and an even-sequence group, so that $r_{ij}^{U_odd}$ and $r_{ij}^{U_even}$ are calculated. Following Eq. (8), the repeatability indicators of the undamaged structure, RI_{ij}^U , are calculated. Similarly, for the damaged structure, the repeatability indicators of the damaged structure, RI_{ij}^D , are calculated. As shown in Figure 5, all repeatability indicators of the experiments for the undamaged and damaged structure are smaller than 0.06. These small repeatability indicators verify that the experimental uncertainties have limited effects to damage detection results.

Damage Scenario II – Loosened Bolts

In Damage Scenario II, four bolts at the upper left corner of the steel frame are loosened (Figure 6). The loosened bolts connect the left end of the beam with the angle plate, which are between locations A3 and A4. The torque of each of the four bolts is reduced from 13.56Nm (120 lbs-in) to 0.565Nm (5lbs-in). Same as previous cases, the two mobile sensors take measurements at location pairs A1-A2, A2-A3,...

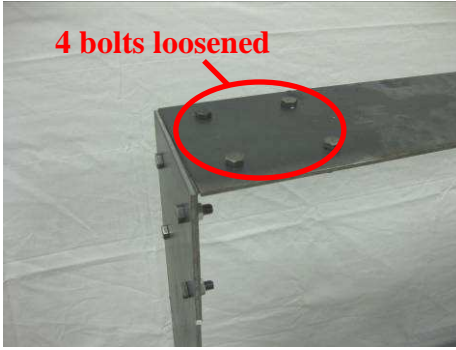


Figure 6. Damage Scenario II - the torque of each of the four bolts is reduced from 13.56Nm (120 lbs-in) to 0.565Nm (5lbs-in). The bolts are between locations A3 and A4.

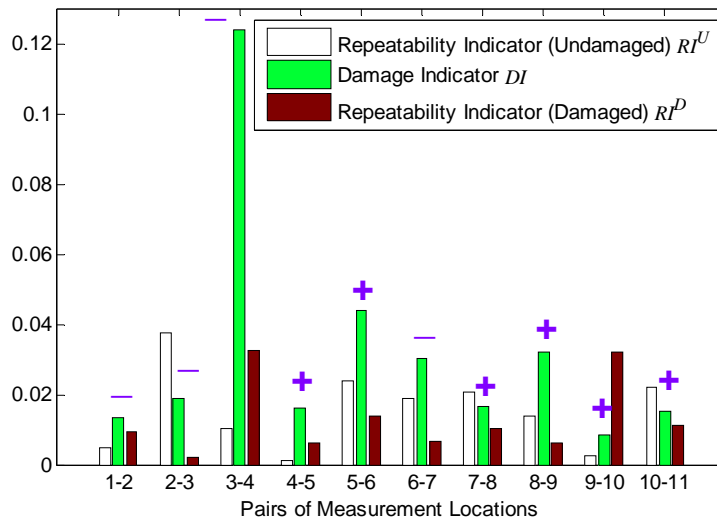


Figure 7. Damage Scenario II - the damage indicators and repeatability indicators for ten pairs of measurement locations. The sign of $r_{ij}^D - r_{ij}^U$ for each location pair is shown above the bar corresponding to the Damage Indicator DI .

and A10-A11, sequentially. At each location pair, the hammer impact experiments are again repeated for 20 times.

The damage indicators as well as the repeatability indicators are calculated and shown in Figure 7. The largest damage indicator is $DI_{3-4} = 0.12$, and the location pair A3 and A4 is the correct damage location where bolts are loosened. Through the sign of $r_{34}^D - r_{34}^U$, it is observed again that for the damaged structure, less similarity exists between the hammer impact responses at location A3 and location A4, when compared with the undamaged structure. In addition, all repeatability indicators of the experiments for the undamaged and damaged structure are less than 0.04, which verify that the experimental uncertainties have limited effects to damage detection.

Damage Scenario III – Loss of Section Area

In Damage Scenario III, reduction in section area is introduced to the left column (Figure 8). The width of the section loss is 0.006 m (0.25 in), and the total length of the loss is $0.0075 + 0.0075 = 0.015$ m (0.6 in),

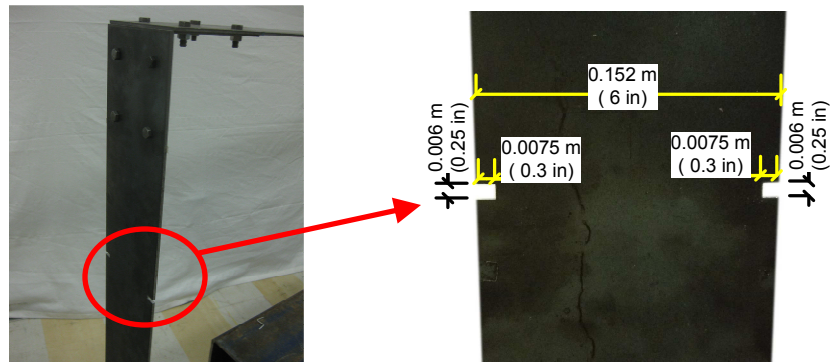


Figure 8. Damage Scenario III – loss in section area is introduced to the left column between locations A2 and A3.

about one tenth of the column width. The location of the section loss is at 0.533 m (21 in) above the column base, which is between locations A2 and A3.

The two mobile sensors again take measurement at location pairs A1-A2, A2-A3, ..., and A10-A11, sequentially, and repeatedly for 20 times at each location pair. The damage indicators as well as the repeatability indicators are calculated and shown in Figure 9. The largest damage indicator is $DI_{2-3} = 0.10$, and the location pair A2 and A3 is the correct damage location where the section area loss are introduced. It is consistently observed that for the location pair (A2 and A3) around the damage, the damaged structure shows less similarity between the hammer impact responses, when compared with the undamaged structure.

In addition, all repeatability indicators of the experiments for the undamaged and damaged structure are less than 0.04, which verifies that the experiments are highly repeatable. Note that the repeatability indicators for the undamaged structure RI_{ij}^U in Figure 9 are different from the repeatability indicators for the undamaged structure RI_{ij}^U in Figure 5 and Figure 7. The reason is that due to the irreversible section loss in Damage Scenario III, a new steel plate is used to replace the left column of the original structure. The measurement for the undamaged structure presented in Figure 9 is retaken with the new plate in place, prior to introducing the section loss for Damage Scenario III.

Conclusion and Future Work

This study explores the application of cross-correlation function for structural damage detection, using vibration data collected by a mobile sensor prototype. A laboratory portal frame is constructed, and three types of damage scenarios (extra mass block, loosened bolts, and section area loss) are investigated. With the acceleration data collected by the mobile sensors, the deterministic cross correlation functions are calculated. By comparing the maximum absolute values of deterministic cross correlation functions of the damaged structure versus the undamaged structure, damage location is accurately determined in all three damage scenarios.

Future work may investigate cross correlation analysis under random excitation input, which can make the methodology more useful for practical applications. Theoretical analysis can be conducted to explain why after damage occurs, the similarity between the impact response at two locations around the damage usually reduces. In addition, mobile excitation nodes can be developed for automatically applying small-magnitude impact forces, so that the mobile sensing and actuation system can operate independently.

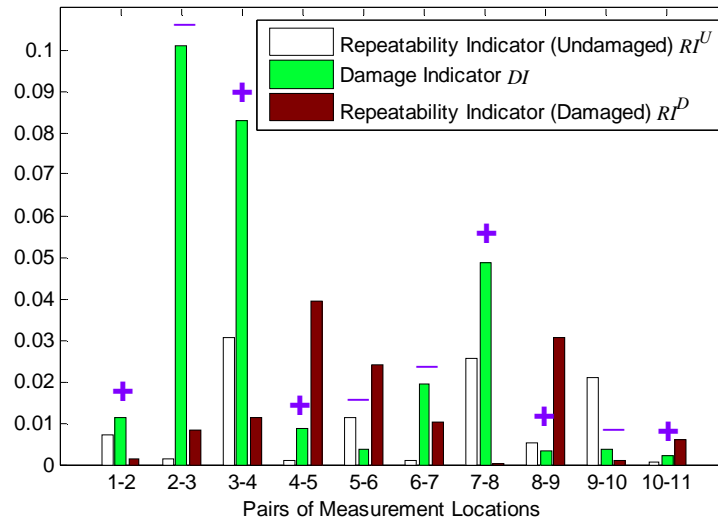


Figure 9. Damage Scenario III - the damage indicators and repeatability indicators for ten pairs of measurement locations. The sign of $r_{ij}^D - r_{ij}^U$ for each location pair is shown above the bar corresponding to the Damage Indicator DI .

Acknowledgements

This research is partially sponsored by the National Science Foundation, under grant number CMMI-0928095 (Program Manager: Dr. Shih-Chi Liu). The authors appreciate the assistance from Dr. Kok-Meng Lee and Mr. Jiajie Guo of the School of Mechanical Engineering at Georgia Institute of Technology, for the development of the mobile sensors.

References

- Akyildiz, I. F., W. Su, Y. Sankarasubramaniam, and E. Cayirci. (2002). "A survey on sensor networks." *Communications Magazine, IEEE*, 40(8), 102-114.
- ASCE. (2009). *Report Card for America's Infrastructure*, American Society of Civil Engineers, Reston, VA.
- Brian, E., M. Jon, R. H. Dryver, and B. Phil. (2004). "Robotic systems for homeland security." *Proceedings of SPIE, Nondestructive Detection and Measurement for Homeland Security II*. San Diego, CA. March 16, 2004.
- Doebbling, S. W., C. R. Farrar, and M. B. Prime. (1998). "A summary review of vibration-based damage identification methods." *The Shock and Vibration Digest*, 30(2), 91-105.
- Farrar, C. R., and G. H. James. (1997). "System identification from ambient vibration measurements on a bridge." *Journal of Sound and Vibration*, 205(1), 1-18.
- Lee, K.-M., Y. Wang, D. Zhu, J. Guo, and X. Yi. (2009). "Flexure-based mechatronic mobile sensors for structure damage detection." *Proceeding of the 7th International Workshop on Structural Health Monitoring*. Stanford, CA. September 9-11, 2009.
- Lin, S. L., J. N. Yang, and L. Zhou. (2005). "Damage identification of a benchmark building for structural health monitoring." *Smart Materials & Structures*, 14(3), S162-S169.
- Lynch, J. P., and K. J. Loh. (2006). "A summary review of wireless sensors and sensor networks for structural health monitoring." *The Shock and Vibration Digest*, 38(2), 91-128.

- Sabra, K. G., E. S. Winkel, D. A. Bourgoyne, B. R. Elbing, S. L. Ceccio, M. Perlin, and D. R. Dowling. (2007). "Using cross correlations of turbulent flow-induced ambient vibrations to estimate the structural impulse response. Application to structural health monitoring." *Journal of the Acoustical Society of America*, 121(4), 1987-1995.
- Tache, F., W. Fischer, G. Caprari, R. Siegart, R. Moser, and F. Mondada. (2009). "Magnebike: A magnetic wheeled robot with high mobility for inspecting complex-shaped structures." *Journal of Field Robotics*, 26(5), 453-476.
- Yang, Z. C., Z. F. Yu, and H. Sun. (2007). "On the cross correlation function amplitude vector and its application to structural damage detection." *Mechanical Systems and Signal Processing*, 21(7), 2918-2932.
- Zhu, D., X. Yi, Y. Wang, K.-M. Lee, and J. Guo. (2010). "A mobile sensing system for structural health monitoring: design and validation." *Smart Materials and Structures*, 19(5), 055011.